Vietnam Journal of Science and Technology ***63*** *(6) (2025) 1094-1106*

doi:10.15625/2525-2518/17649

Effects of inorganic fillers on the performance of acrylic emulsion intumescent fire retardant coating

Nguyen Anh Hiep*, Dao Phi Hung, Mac Van Phuc, Nguyen Thien Vuong, Trinh Van Thanh

Institute of Materials Science, Vietnam Academy of Science and Technology, 18 Hoang Quoc Viet, Nghia Do, Ha Noi, Viet Nam

*Email: *anhhiepvktnd@gmail.com*

Received: 11 November 2022; Accepted for publication: 6 March 2023

Abstract. This study investigates the influence of $CaCO_3$ and talc powders on the performance of a water-based intumescent fire-retardant coating. The coatings were evaluated through Bunsen burner and furnace fire tests, water immersion, SEM, TGA, DSC, and mechanical property measurements. Both fillers reduced the intumescent factor, with talc exerting a stronger suppressing effect than $CaCO_3$; however, they enhanced fire resistance and thermal stability. The formulation in which 5 wt.% $CaCO_3$ replaced conventional fillers ($Al(OH)_3$ and TiO_2) exhibited the highest fire resistance, achieving a backside temperature of only 165 °C after 60 minutes of fire exposure. Despite its superior fire protection, this coating showed markedly poor water resistance, with a weight loss of 14.77 % after 7 days of immersion, compared with 3.28 % for the conventional formulation. Overall, the results confirm that while $CaCO_3$ and talc can strengthen fire resistance and thermal stability, they negatively affect the expansion behavior of the intumescent system. In particular, incorporating 5 wt.% $CaCO_3$ offers significant fire-retardant benefits but compromises water durability, highlighting the need for optimized filler selection in water-based intumescent coatings.

Keywords: Intumescent coating, acrylic emulsion, inorganic fillers, fire resistance, thermal degradation.

Classification numbers: 2.5.3

1. INTRODUCTION

Fire safety for building structures requires not only limiting flame spread but also maintaining structural integrity during fire exposure. Intumescent coatings swell under high temperatures to form an insulating char foam that protects the substrate, increases evacuation time, and reduces post-fire repair costs [1, 2]. A typical intumescent system includes a polymer binder and flame-retardant additives: an acid source (APP), a carbon source (PER), and a blowing agent (MEL). When heated above 250 °C, APP releases phosphoric acid, which reacts with PER to form a carbonized layer, while MEL decomposes to release non-combustible gases that expand the viscous matrix into a multicellular protective char with low thermal conductivity [3, 4].

However, char produced by the APP–PER–MEL system shows weak oxidation resistance at high temperatures, reducing flame-retardant efficiency [5]. Mineral fillers such as $CaCO_3$,

silica, $Mg(OH)_2$, and $Al(OH)_3$ are therefore used to enhance thermal shielding and char compactness [6]. TiO_2 also stabilizes the char at elevated temperatures and may form titanium pyrophosphate with low thermal conductivity; rutile TiO_2 provides better thermal stability than anatase [7]. Metal hydroxides, especially $Al(OH)_3$, act through endothermic decomposition and water release, which dilute combustible gases [8].

Talc ($Mg_3Si_4O_{10}(OH)_2$) improves film strength and withstands heating up to 800 °C. Studies show that talc enhances swelling, water resistance, and fire performance by forming a ceramic-like protective layer [9, 10]. $CaCO_3$ is also a widely used filler that improves mechanical strength and contributes to fire resistance [11, 12]. Among binders, water-based acrylic emulsions are preferred for environmental compatibility and good durability [6, 13].

This study evaluates the effects of talc and $CaCO_3$ on the fire resistance, thermal behavior, and mechanical properties of an acrylic-based waterborne intumescent coating containing APP, MEL, PER, TiO_2, and $Al(OH)_3$.

2. MATERIALS AND METHODS

2.1. Materials

Acrylic emulsion Plextol R4152 (49 ± 1 % solid content, pH 7 - 8.5) was supplied by Synthomer. APP and PER were purchased from CF-Chem Co., Ltd., while MEL was obtained from Hangzhou JLS Flame Retardant Chemical Co., Ltd. Aluminium hydroxide and rutile titanium dioxide were provided by Aladdin Industrial Co., Ltd. Talc powder was sourced from Indian Chemical Co., Ltd., and $CaCO_3$ from Xilong. Triton X-405 (70 %) surfactant was purchased from Sigma Aldrich, and Texanol coalescing agent from Dow Chemical Co. Drewplus T 4507A defoamer was supplied by Ashland Global Holdings Inc. Deionized water was prepared in the laboratory.

2.2. Sample preparation

The coating formulations are presented in Table 1, with the filler content fixed at 10 wt.%.

Table 1. The components of the coatings (wt.%).

No	*Components*	*S1*	*S2*	*S3*	*S4*	*S5*	*S6*
1	R4152 acrylic emulsion polymer	38	38	38	38	38	38
2	APP/PER/MEL	18/9/9	18/9/9	18/9/9	18/9/9	18/9/9	18/9/9
3	TiO_2	5	-	2.5	-	2.5	2.5
4	$Al(OH)_3$	5	-	2.5	-	2.5	2.5
5	Talc	-	10	5	-	-	2.5
6	$CaCO_3$	-	-	-	10	5	2.5
7	Distilled water	15	15	15	15	15	15
8	Additives (surfactant, coalescing, foam control)	1	1	1	1	1	1

The intumescent coatings were prepared as follows. First, the flame-retardant additives (APP, PER, MEL), fillers, and surfactant were mixed using a high-speed stirrer (IKA RW16 Basic) at 1200 rpm for 1 hour. Subsequently, the acrylic emulsion R4152 and other additives (coalescing agent and defoamer) were added to the slurry and stirred for an additional 1 hour at 500 rpm. The

resulting coatings were applied onto SS400 steel plates previously cleaned with sandpaper and acetone, then dried at ambient conditions for seven days. The dry coating thickness was controlled within 1.3 ± 0.1 mm and measured using a Mitutoyo 500-150-30 digital caliper.

2.3. Analysis

2.3.1. Fire resistance test

The fire resistance of the coatings was evaluated using a Bunsen burner test, as illustrated in Figure 1. The coatings were applied onto SS400 steel plates with dimensions of 150 mm × 150 mm × 5 mm. Each sample was exposed to a Bunsen burner flame for 1 hour, with the flame temperature maintained at approximately 800 - 1000 °C and the burner positioned 7 cm from the specimen surface. During the test, the backside temperature of the steel plate was continuously monitored using a Testo 925 type-K thermometer (Testo AG, Germany).

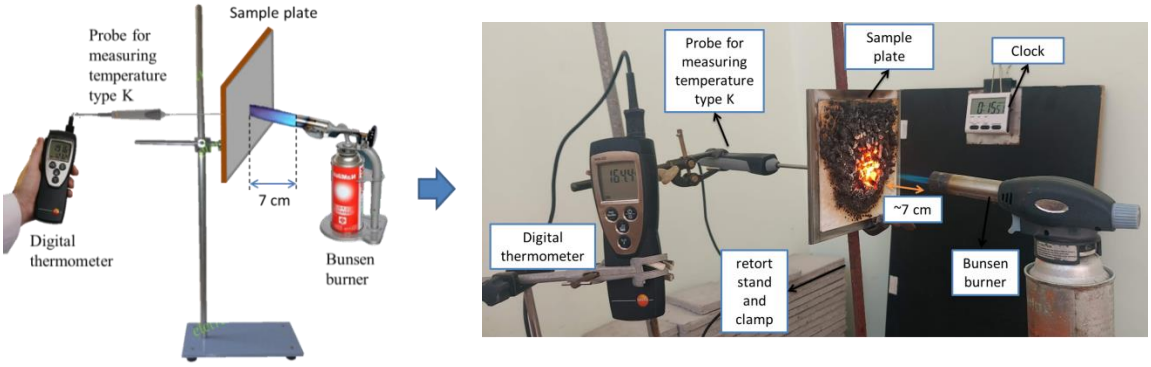

Figure 1. Schematic of the experimental setup for fire resistance test.

2.3.2. Furnace test

The furnace test was conducted to evaluate the swelling behavior of the intumescent coatings. Steel plates with dimensions of 100 mm × 100 mm × 5 mm were coated and subjected to a programmed heating cycle, in which the temperature increased from room temperature to 800 °C at a rate of 10 °C/min. The temperature was maintained at 800 °C for 30 minutes and then allowed to cool to room temperature. The intumescent factor (I) was determined from the change in coating thickness before and after the furnace test. It was calculated using the following Equation 1:

$$I = d_2 / d_1 \quad (1)$$

where d_1 is the thickness of the coating before the furnace test, d_2 is the thickness of the char layer after the furnace test.

The coating and char layer thickness was measured with a Mitutoyo 500-150-30 digital caliper.

2.3.3. Morphology

The morphological structure of coatings and char layer was observed using a scanning electron microscope (SEM) JSM-6510LV (Jeol Company - Japan).

2.3.4. Thermogravimetric analysis (TGA)

Thermogravimetric analysis was determined by TGA 209F1 (NETZSCH - Germany). The

sample was heated from ambient temperature to 800 ^{o}C at heating rate of 10 ^{o}C/min in the air.

2.3.5. Differential scanning calorimetry (DSC)

Differential scanning calorimetry was determined using DSC204F1 (NETZSCH - Germany) in the air with a heating rate of 20 ^{o}C/min from room temperature to 400 ^{o}C.

2.3.6. Static immersion test

Static immersion tests were conducted to evaluate the water resistance of the coatings. Samples were cast in a silicone mold to form bars measuring 50 mm × 20 mm × 2 mm and dried for one week before demolding. The specimens were then immersed in distilled water at room temperature and removed at designated time intervals. Excess surface water was gently wiped off with tissue paper. The water uptake ratio (E_{sw}) of each sample was determined using Equation 2:

$$E_{sw}\,(\%) = [(W_a - W_b)/W_b] \times 100\% \quad (2)$$

where W_b is the weight of the coating sample before the water immersion test (g), and W_a is the dry weight of the coating sample under the water immersion test (g).

2.3.7. Mechanical properties

- *Adhesion strength:* The adhesion strength of the coatings on the concrete substrate was evaluated using a pull-off adhesion tester (PosiTest AT-A Automatic, DeFelsko) in accordance with ASTM D4541. The coatings were applied on the concrete plate with 1 ± 0.1 mm thickness.

- *Pendulum hardness*: The pendulum hardness of the coatings was measured using a Pendulum Damping Tester (model 299/300, Erichsen) following ASTM D4366. The coatings were applied onto glass plates using a Film Applicator (model 306, Erichsen) with a wet thickness of 120 µm. The pendulum hardness was calculated as the ratio of the number of oscillations on the coated glass to that on the reference glass..

3. RESULTS AND DISCUSSION

3.1. Fire resistance test

Fire resistance is a critical performance indicator for intumescent coatings. The fire resistance of coatings with different filler types and contents is presented in Figure 2, and the corresponding post-fire surface morphologies are shown in Figure 3.

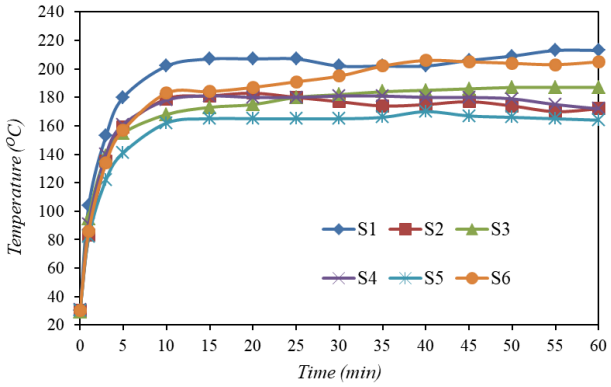

Figure 2. Effect of type and content of fillers on the fire resistance of the coating.

As illustrated in Figure 2, the backside temperature of all samples rose rapidly above 160 °C during the first 10 minutes, followed by a slower increase. This behavior is attributed to thermal degradation and the formation of a protective char layer through chemical reactions among coating components [14]. Most coatings reached an equilibrium temperature after approximately 15 minutes, except for samples S3 and S6, which continued to heat up and stabilized at around 200 °C after 35 minutes.

Overall, the incorporation of talc (S2, S3) and $CaCO_3$ (S4, S5) enhanced the fire resistance of the coatings by reducing the heat transfer to the steel substrate. Among all samples, S5 exhibited the best performance. After 60 minutes of flame exposure, the backside temperatures of the coatings followed the descending order: S1 (213 °C) > S6 (205 °C) > S3 (187 °C) > S2 ≈ S4 (173 °C) > S5 (165 °C).

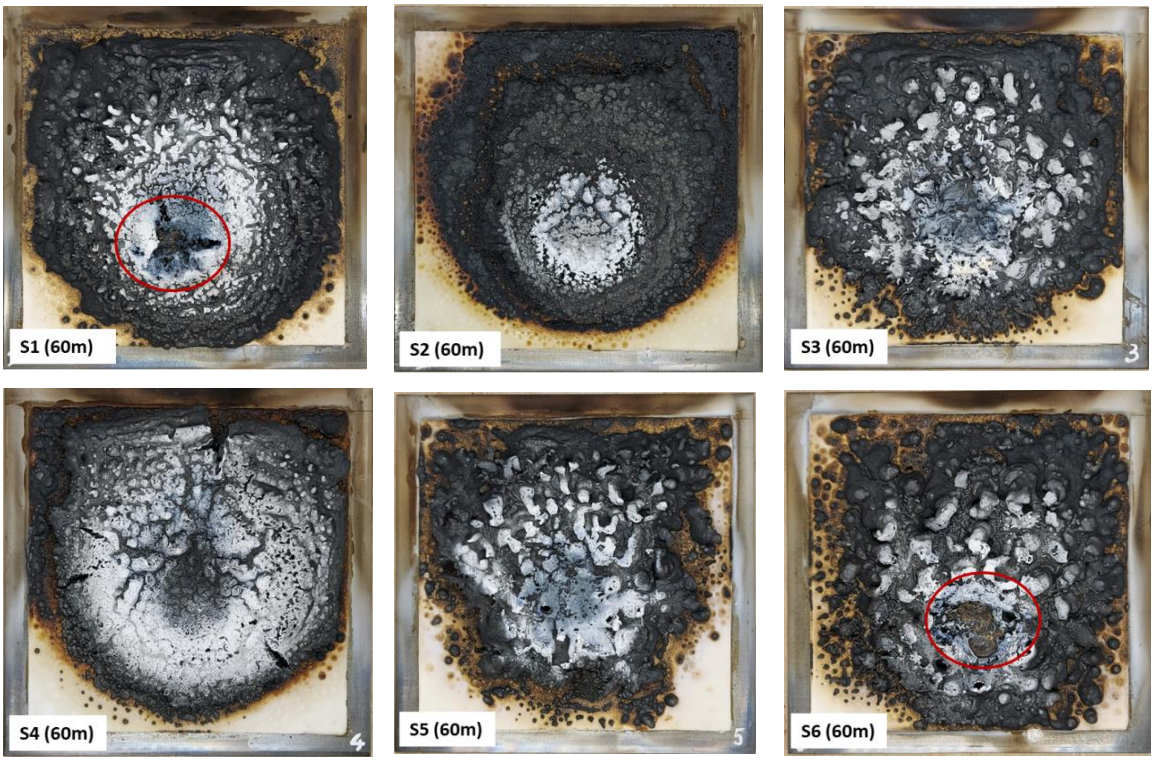

Figure 3. The photographs of coatings after 60 minutes of the fire resistance test.

As shown in Figure 3, after 60 minutes of fire exposure, the char layers of samples S1 and S6 exhibited clear cracking and collapse at the points of direct flame contact (indicated in red). In contrast, the remaining samples showed no significant cracks or structural failure. The damaged char of S1 and S6 exposed the steel substrate to the flame, resulting in greater heat transfer and therefore the highest backside temperatures among all samples.

The improved fire resistance observed in the other formulations can be attributed to the endothermic decomposition of the flame-retardant fillers $Al(OH)_3$, talc, and $CaCO_3$ at elevated temperatures. Their decomposition releases water vapor or CO_2, which dilutes combustible degradation products of the polymer matrix while leaving behind thermally stable inorganic residues. This process reduces the effective flame temperature and slows heat transmission to the substrate. The endothermic decomposition reactions of the fillers are described by the following

equations [12]:

$$2Al(OH)_{3\,(s)} \rightarrow Al_2O_{3\,(s)} + 3H_2O_{\,(g)} \quad (3)$$

$$Mg(OH)_{2\,(s)} \rightarrow MgO_{(s)} + H_2O_{\,(g)} \quad (4)$$

$$CaCO_{3\,(s)} \rightarrow CaO_{\,(s)} + CO_{2\,(g)} \quad (5)$$

3.2. Furnace test

The furnace test was carried out to check the formation of the char layer at 800 ℃ and to determine the intumescent factor *I* of the coatings, as shown in Figure 4. Images of the initial coatings and after the furnace test are presented in Figure 5.

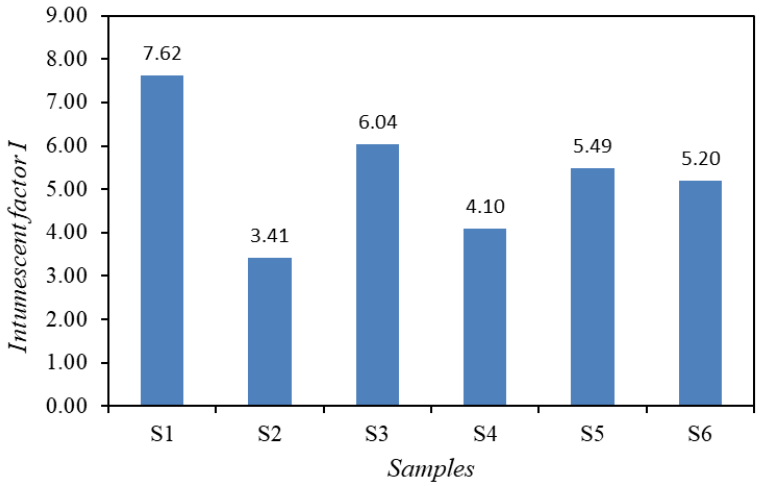

Figure 4. The intumescent factor *(I)* of the coating samples.

Figure 4 shows that sample S1 (without talc or $CaCO_3$) exhibits the greatest swelling among all coatings. However, a higher intumescent factor does not necessarily correspond to better fire resistance. Although swelling is important for thermal insulation, fire protection efficiency also depends on factors such as filler morphology, chemical structure, distribution, and thermal properties [15].

The cross-section of S1 reveals large voids, which result in a thinner and more fragile char surface prone to cracking. A similar structure is observed in S6; with only 2.5 wt.% talc and 2.5 wt.% $CaCO_3$, the filler content appears insufficient. This observation is consistent with the cracking and collapse seen in the fire resistance test (Section 3.1). In contrast, samples S2, S3, S4, and S5 show denser, lower-expansion, and less porous char layers (Figure 5). This improvement is likely due to the higher filler content (5 - 10 wt.%), which promotes the formation of a more compact and stable char while reducing excessive swelling.

Some studies showed that talc filler had good insulation properties due to the silicate layer "foam" on char, like a ceramic layer to protect the underlying substrate [9, 10]. The fillers (talc, $CaCO_3$) have a high melting point, making the coating withstand high temperatures. However, this hinders the release and diffusion of the gases produced during the combustion process, leading to limited swelling of the char layer. To clarify this issue further, it is necessary to further analyze the morphology of the char layer through SEM analysis.

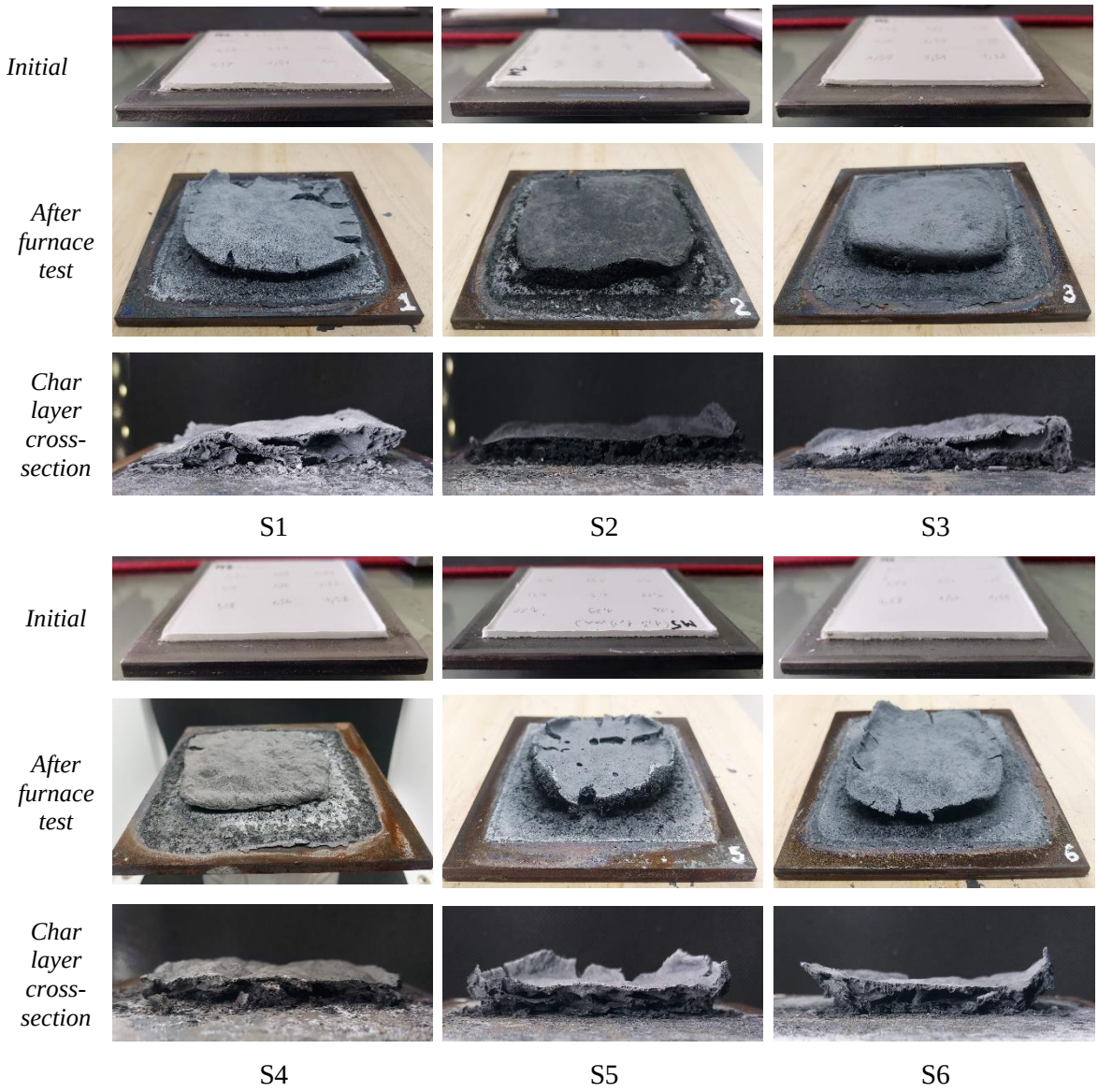

Figure 5. Images of the initial coatings and after furnace test.

3.3. Morphology of coatings and char layer

SEM images of the cross-sections of the investigated coatings at 10,000× magnification are presented in Figure 6. As observed, samples S2, S4, and S5 exhibit good filler dispersion, forming uniform and continuous structures. In contrast, samples S1, S3, and S6 show visible cracks and voids, which correlate with their lower fire resistance performance in the Bunsen burner test (Section 3.1).

The fire resistance of intumescent coatings is strongly influenced by the structure of the char layer. A dense and compact char serves as an effective thermal barrier between the flame and the substrate, thereby enhancing fire protection [16]. The SEM micrographs of the char layers after the furnace test are shown in Figure 7. For samples S1 (0 wt.% talc, 0 wt.% $CaCO_3$),

S3 (5 wt.% talc), and S6 (2.5 wt.% talc and 2.5 wt.% $CaCO_3$), numerous cracks and voids were observed in the char structure. These defects facilitated the penetration of heat and flame toward the steel substrate, resulting in reduced fire resistance.

In contrast, the SEM images of samples S2 (10 wt.% talc), S4 (10 wt.% $CaCO_3$), and S5 (5 wt.% $CaCO_3$) revealed a denser and more compact char morphology, characterized by fewer and smaller cracks. This improved structural integrity contributed to enhanced thermal insulation during the fire resistance test. Overall, the relatively homogeneous and dense char layers of these samples acted as an effective protective barrier, thereby improving the insulation performance of the coating system [9].

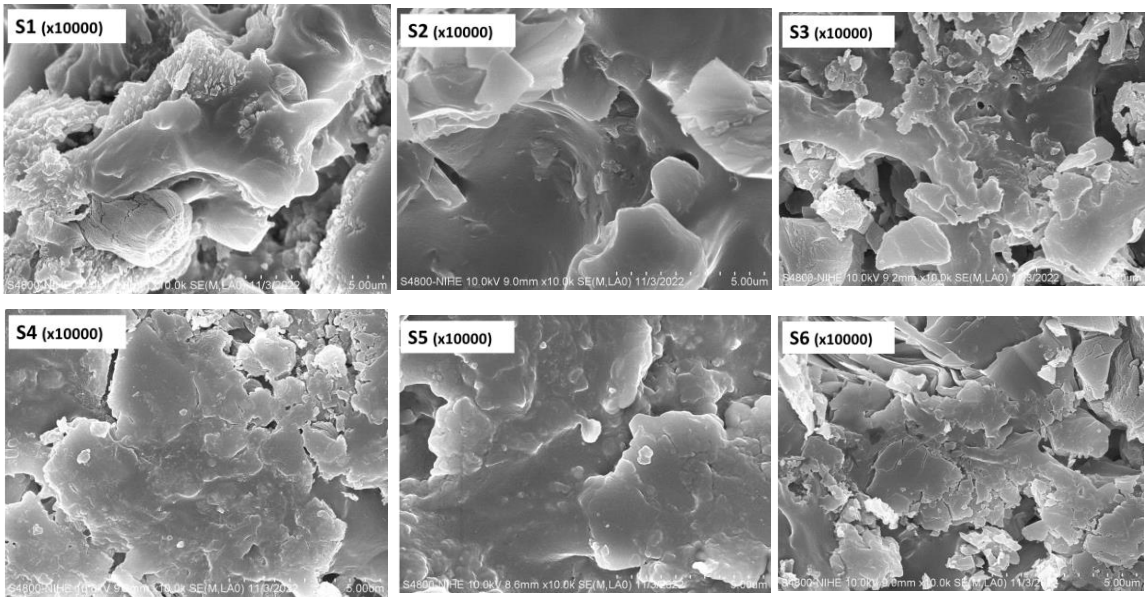

Figure 6. SEM micrographs of the cross-section of the coating.

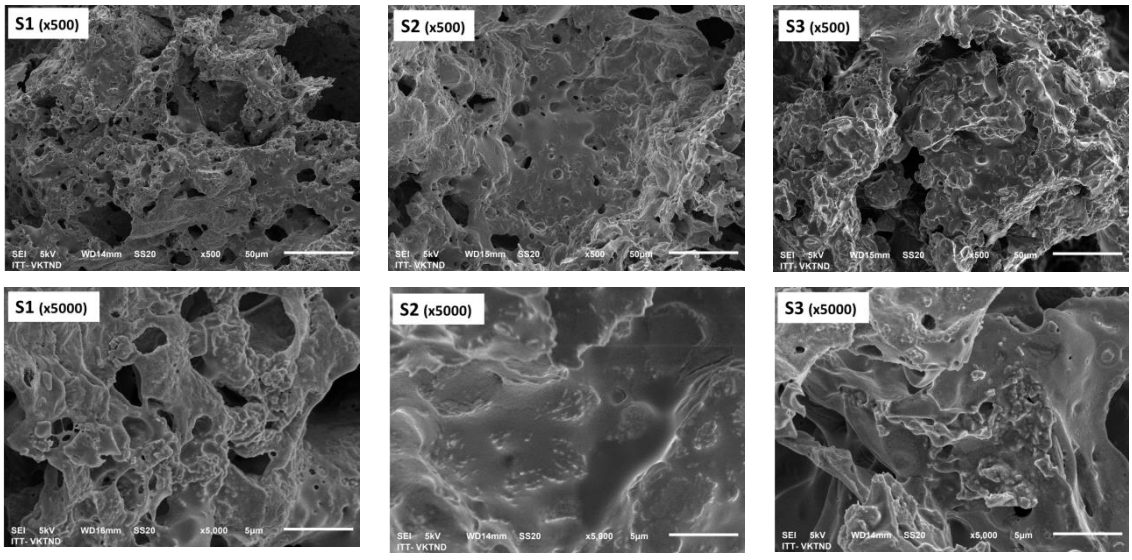

Figure 7. SEM micrographs of the char layer cross-section

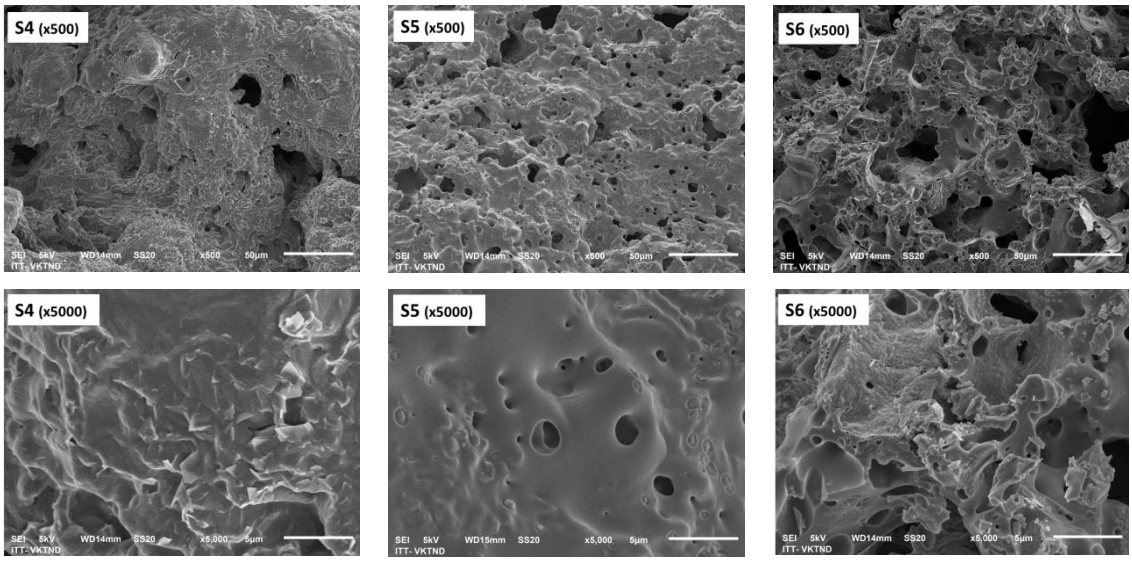

Figure 7. SEM micrographs of the char layer cross-section (continue).

3.4. TGA-DSC analysis

Thermogravimetric analysis (TGA) was conducted to examine the thermal stability and degradation behavior of the coatings. Samples S1, S3, S5, and S6 were selected for this test, and their TGA curves are shown in Figure 8.

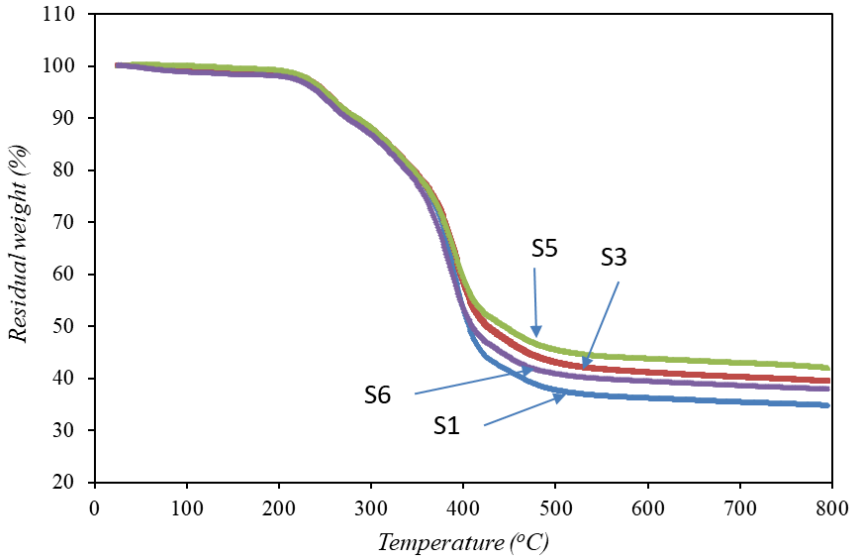

Figure 8. TGA curve of the coatings.

According to Figure 8, all coating samples exhibited similar thermal degradation profiles, consisting of three main stages. In the first stage, from ambient temperature to 200 °C, the coatings experienced a weight loss of approximately 1 – 2 %, corresponding to the evaporation of residual moisture and small volatile molecules from the binder.

The second stage occurred between 200 °C and 500 °C, where a rapid weight loss was

observed. During this stage, APP decomposes and releases NH_3 and water vapor in the temperature range of 250 - 350 °C, initiating the swelling process of the intumescent coating [17]. At around 350 °C, the samples exhibited a weight reduction of approximately 20 %, which is likely attributable to the decomposition of APP—the component accounting for about 18 wt.% of the coating formulation. In addition, the resin matrix begins to soften within this temperature range, while MEL releases gases that contribute to the foaming process, along with the thermal degradation of the outer coating layer [7].

In the final stage, from 500 to 800 °C, the weight loss of the samples became relatively stable as carbonaceous structures were gradually formed and consumed [5]. At 800 °C, sample S1 (0 wt.% talc, 0 wt.% $CaCO_3$) exhibited the lowest residual mass at approximately 34.71 %. Meanwhile, the residual weights of samples S3 (5 wt.% talc), S6 (2.5 wt.% talc and 2.5 wt.% $CaCO_3$), and S5 (5 wt.% $CaCO_3$) were 37.84 %, 39.36 %, and 41.97 %, respectively. The higher residual masses indicate that the incorporation of talc and $CaCO_3$ enhances the thermal stability of the coatings, contributing to improved fire resistance during combustion.

Differential scanning calorimetry (DSC) was performed on samples S1 and S6 to further investigate their decomposition behavior. The DSC curves are presented in Figure 9.

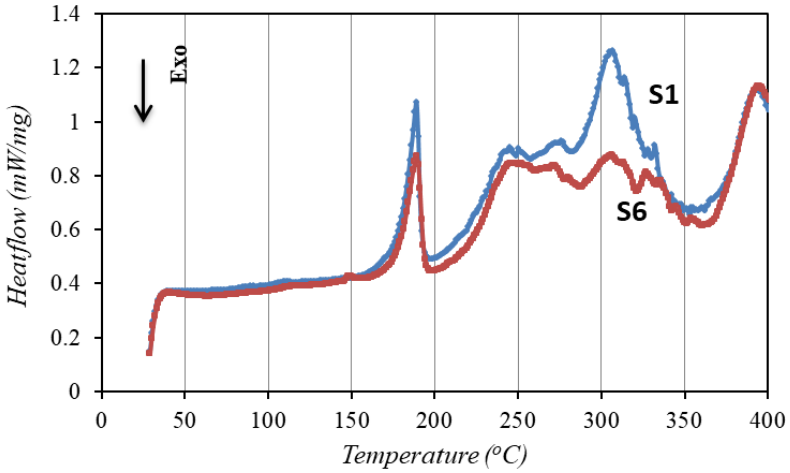

Figure 9. DSC curve of S1 and S6 coating samples.

As shown, a small endothermic peak appears at approximately 150 °C, corresponding to the initial melting of the acrylic resin. In the temperature range of 170–200 °C, an endothermic peak at around 188 °C is observed, which is attributed to the melting of APP and the crystal structure transformation of PER. A larger endothermic peak appears between 240 °C and 290 °C. This peak is associated with the onset of APP decomposition above 250 °C, during which phosphoric acid and amines are released. In this temperature range, PER also begins to decompose and reacts with the generated phosphoric acid to promote char formation. Above 300 °C, MEL starts to decompose, releasing non-flammable gases such as CO_2 and N_2. These gases become trapped within the viscous matrix and form bubbles, resulting in a blistered structure that expands into a protective char layer. This char layer effectively insulates the underlying substrate by creating a multi-compartment barrier between the flame and the coating surface [5,18].

3.5. Static immersion test

Figure 10 shows the mass-change profiles of the coatings during 7 days of immersion in

distilled water. After two days of immersion, the coating weight increased by approximately 5–15%, followed by a gradual decrease in the subsequent days.

During the static immersion test, two simultaneous processes occur: permeation and migration. Depending on the immersion duration, one of these processes becomes dominant. In the permeation process, water and corrosive ions penetrate the coating through its pores, leading to an increase in coating mass. Concurrently, some hydrophilic flame-retardant components (APP, PER, and MEL) migrate from the coating into the surrounding water, resulting in mass loss [18].

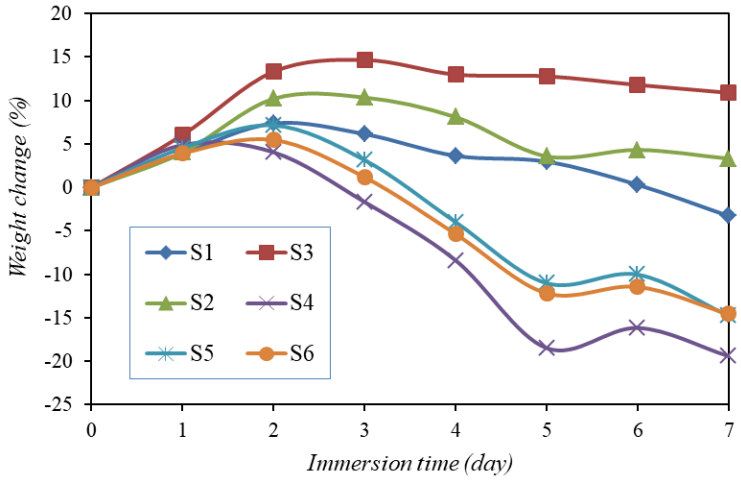

Figure 10. The weight change of the coatings over time of static immersion test.

In the first two days of the test, the permeation of water molecules dominated the migration of hydrophilic flame retardants, resulting in an overall increase in coating mass. In the following days, the migration process prevailed over permeation, causing the mass to decrease. After 7 days of immersion, no mass loss was observed for samples S2 and S3, which contained 10 wt.% and 5 wt.% talc fillers, respectively. This confirms that the water repellence of the coatings improved with increasing talc content. The lamellar structure and hydrophobic nature of talc, which is insoluble in water, help restrict water uptake by the coating [9].

In contrast, samples S4, S5, and S6 containing 10, 5, and 2.5 wt.% $CaCO_3$ fillers, respectively, exhibited weight loss after 3 days of immersion. In this case, apart from the migration of hydrophilic flame retardants, $CaCO_3$ also reacted with water containing dissolved CO_2 to form water-soluble calcium bicarbonate:

$$CaCO_3 + CO_2 + H_2O \rightarrow Ca(HCO_3)_2 \quad (6)$$

The S1 sample also showed a tendency to lose weight after 6 days of immersion due to the migration of hydrophilic flame-retardant components. The weight reductions of samples S1, S4, S5, and S6 after 7 days were 3.28 %, 19.40 %, 14.77 %, and 14.55 %, respectively.

3.6. Mechanical properties of coatings

The pendulum hardness and adhesion strength of the coatings were evaluated to determine the influence of the fillers on the mechanical properties of the coating system. The experimental results are summarized in Table 2.

Table 2. Pendulum hardness and adhesion of the investigated coatings.

Properties	*S1*	*S2*	*S3*	*S4*	*S5*	*S6*
Pendulum hardness	0.31	0.30	0.33	0.31	0.34	0.30
Adhesion (MPa)	4.18	4.21	4.53	4.32	4.61	4.0

It can be seen from that Table 2 the combination of fillers $Al(OH)_3$, TiO_2 with talc (S3 sample) and $CaCO_3$ (S5 sample) helps to increase hardness from 6.5 % - 9.7 % and adhesion from 8.4 % - 10.3 % compared to sample S1. However, combining all four fillers in the S6 sample reduced the mechanical properties. This result can be explained by weak interfacial compatibility between the components. The cross-sectional SEM image of the S6 coating sample (Figure 6) showed cracks, holes and delamination.

4. CONCLUSIONS

This study demonstrates that adding talc and $CaCO_3$ significantly affects the performance of the acrylic-based intumescent coating. Although both fillers reduce the intumescent factor, they enhance fire resistance compared to conventional fillers. The formulation containing 5 wt.% $CaCO_3$ exhibited the best performance, reaching only 165 °C on the backside after 60 minutes of fire exposure. $CaCO_3$ also improved the coating's adhesion and hardness, though it reduced water resistance. Overall, $CaCO_3$ is a promising filler for enhancing the fire protection efficiency and mechanical properties of acrylic intumescent coatings.

Acknowledgments. This work received support from the Annual Financial Fund of the Vietnam Academy of Science and Technology.

Authorship contribution*:* Nguyen Anh Hiep: Investigation, Writing - Original Draft; Dao Phi Hung: Methodology, Writing - Review & Editing; Mac Van Phuc: Conceptualization, Project administration, Funding acquisition; Nguyen Thien Vuong: Data Curation; Trinh Van Thanh: Validation.

Declaration of competing interest. The authors declare no competing interests.

REFERENCES

1. Edward D. Weil - Fire-Protective and Flame-Retardant Coatings - A State-of-the-Art Review. Journal of Fire Sciences **29** (3) (2011) 259-296.
2. Muhammad Yasir, Faiz Ahmad, Puteri Sri Melor Megat Yusoff, Sami Ullah and Maude Jimenez - Latest trends for structural steel protection by using intumescent fire protective coatings: a review. Surface Engineering **36** (2) (2019) 1-30.
3. Guojian Wang, Jiayun Yang - Influences of binder on fire protection and anticorrosion properties of intumescent fire resistive coating for steel structure. Surface and Coatings Technology **204** (8) (2010) 1186-1192.
4. Hongfei Li, Zhongwu Hu, Sheng Zhang, Xiaoyu Gu, Huajin Wang, Peng Jiang and Qian Zhao- Effects of titanium dioxide on the flammability and char formation of water-based coatings containing intumescent flame retardants. Progress in Organic Coatings **78** (2015) 318-324.
5. Yadong Xue, Shiping Zhang, Wenliang Yang - Influence of expanded vermiculite on fire protection of intumescent fireproof coatings for steel structures. Journal of Coatings Technology and Research **12** (2) (2015) 357-364.

6. Khairunisa Md Nasir, Nor Hafizah Ramli Sulong, Mohd Rafie Johan and Amalina M. Afifi - Synergistic effect of industrial- and bio-fillers waterborne intumescent hybrid coatings on flame retardancy, physical and mechanical properties, Progress in Organic Coatings **149** (2020) 105905.
7. Thirumal Mariappan, Aishvarye Agarwal, Sushma Ray - Influence of titanium dioxide on the thermal insulation of waterborne intumescent fire protective paints to structural steel, Progress in Organic Coatings **111** (2017) 67-74.
8. Khairunisa Md Nasir, Nor Hafizah Ramli Sulong, Talal Fateh, Mohd Rafie Johan and Amalina Muhammad Afifi - Combustion of waterborne intumescent flame-retardant coatings with hybrid industrial filler and biofiller, Journal of Coatings Technology and Research **16** (2019) 543–553.
9. H. Hazwani Dzulkafli, Faiz Ahmad, Sami Ullah, Patthi Hussain, Othman Mamat and Puteri S.M. Megat-Yusoff - Effects of talc on fire retarding, thermal degradation and water resistance of intumescent coating, Applied Clay Science **146** (2017) 350-361.
10. X. Almeras, M. Le Bras, F. Poutch, S. Bourbigot, G. Marosi and P. Anna - Effect of fillers on fire retardancy of intumescent polypropylene blends, Macromolecular Symposia **198** (2003) 435-447.
11. Jessica Jong Kwang Yin,Ming Chian Yew, Ming Kun Yew and Lip Huat Saw - Preparation of intumescent fire protective coating for fire rated timber door, Coatings **9** (11) (2019) 738.
12. Khairunisa Md Nasir, Nor Hafizah Ramli Sulong, Mohd Rafie Johan and Amalina Muhammad Afifi - An investigation into waterborne intumescent coating with different fillers for steel application, Pigment and Resin Technology **47** (2) (2018) 142-153.
13. Dao Phi Hung, Vo An Quan, Trinh Van Thanh, Nguyen Anh Hiep, Nguyen Thien Vuong and Mac Van Phuc - Mechanical, thermal properties and morphology of composite coating based on acrylic emulsion polymer and graphene oxide, Vietnam Journal of Science and Technology **58** (2) (2020) 228-236.
14. Hammad Aziz, Faiz Ahmad - Effects from nano-titanium oxide on the thermal resistance of an intumescent fire retardant coating for structural applications, Progress in Organic Coatings **101** (2016) 431-439.
15. Mohammadreza Nasirzadeh, Hossein Yahyaei, Mohsen Mohseni - Effects of inorganic fillers on the performance of the water-based intumescent fire-retardant coating, Fire and Materials **47** (1) (2022) 51-61.
16. Zhenyu Wang, Enhou Han, Wei Ke - Effect of nanoparticles on the improvement in fire-resistant and anti-ageing properties of flame-retardant coating, Surface and Coatings Technology **200** (20) (2006) 5706-5716.
17. Jun-wei Gu, Guang-cheng Zhang, Shan-lai Dong, Qiu-yu Zhang and Jie Kong - Study on preparation and fire-retardant mechanism analysis of intumescent flame-retardant coatings, Surface and Coatings Technology **201** (18) (2007) 7835-7841.
18. Wang Zhan, Le Chen, Fusheng Cui, Zhaozhan Gu and Juncheng Jiang - Effects of carbon materials on fire protection and smoke suppression of waterborne intumescent coating, Progress in Organic Coatings **140** (4) (2020) 105491.